Glass Transition for Driven Granular Fluids

W. Till Kranz,[1,2] Matthias Sperl,[3] and Annette Zippelius[2,1]

[1]*Max-Planck-Institut für Dynamik und Selbstorganisation, Bunsenstrasse 10, 37073 Göttingen, Germany*
[2]*Georg-August-Universität Göttingen, Institut für Theoretische Physik, Friedrich-Hund-Platz 1, 37077 Göttingen, Germany*
[3]*Institut für Materialphysik im Weltraum, Deutsches Zentrum für Luft-und Raumfahrt, 51170 Köln, Germany*

(Received 10 February 2010; published 1 June 2010)

We investigate the dynamics of a driven system of dissipative hard spheres within mode-coupling theory. The dissipation is modeled by normal restitution, and driving is applied to individual particles in the bulk. In such a system, a glass transition is predicted for a finite transition density. With increasing dissipation, the transition shifts to higher densities. Despite the strong driving at high dissipation, the transition persists up to the limit of totally inelastic normal restitution.

DOI: 10.1103/PhysRevLett.104.225701 PACS numbers: 64.70.ps, 61.20.Lc, 64.70.Q−

The jamming diagram of Liu and Nagel [1] conjectures for the space spanned by the parameters packing fraction φ, temperature T, and external stress σ, that there is a region where the material is solidlike (or jammed), cf. Fig. 1. This perspective unifies the concepts of jamming for macroscopic, athermal particles and of the glass transition for microscopic, thermal particles. A lot of work has been devoted to point J—the arrest of quasistatic granular assemblies [2]. Similarly, the glass transition of a supercooled molecular liquid has been studied extensively, corresponding to a transition line in the φ-T plane, which in the case of hard spheres is parallel to the T axis. In such a system of elastic hard spheres, the glass transition is described well by mode-coupling theory (MCT) [3,4]. Whether a unified picture of the jamming diagram holds, however, is still a matter of debate.

It was shown by theory and computer simulation that both Newtonian and Brownian equations of motion yield the same glassy dynamics [5–7]. The situation is different when the system is subject to shear. A recent extension of MCT for this case shows for colloidal suspensions that any finite shear rate is able to destroy the glass transition [8]. While remnants of the glass transition still affect the dynamics, full arrest is no longer possible. Another scenario is proposed by the mentioned jamming diagram where applied shear stress unjams the system but can be compensated for with a higher density or lower temperature, cf. Fig. 1(a).

It is the objective of the present Letter to investigate the possibility of a glass transition in a granular fluid at steady state when dissipation is balanced by bulk driving. Experiments by Abate and Durian [9] and Reis *et al.* [10] showed indications of a granular glass transition in such fluidized granular systems in two dimensions. These observations would fit into a modified jamming diagram, where the axis shear-stress σ is replaced by the driving force v_{dr} used to compensate for the dissipation among the granular particles. In the following, we shall investigate if a granular glass transition can exist at a finite kinetic temperature and how such a transition can be described by an appropriate theory. It will be demonstrated that (1) the combination of MCT [6] with granular kinetic theory [11] predicts a glass transition for a driven dissipative system, (2) the nature of the transition depends on the degree of dissipation, and (3) granular dynamics cannot be scaled onto Brownian or Newtonian dynamics.

We consider the nonequilibrium stationary state of a driven granular fluid comprised of N frictionless hard spheres of diameter d and mass m in a volume V at number density $n = N/V$. Energy dissipation in binary collisions is modeled by a coefficient of normal restitution ε. Because of the energy loss in the collisions the system needs to be driven in order to achieve a stationary state. We use a simple bulk driving mechanism, e.g., as in air fluidized beds [9]. The particles are kicked

$$\boldsymbol{v}_i'(t) = \boldsymbol{v}_i(t) + v_{\mathrm{dr}}\boldsymbol{\xi}_i(t)$$

with frequency ω_{dr} which is taken comparable to the

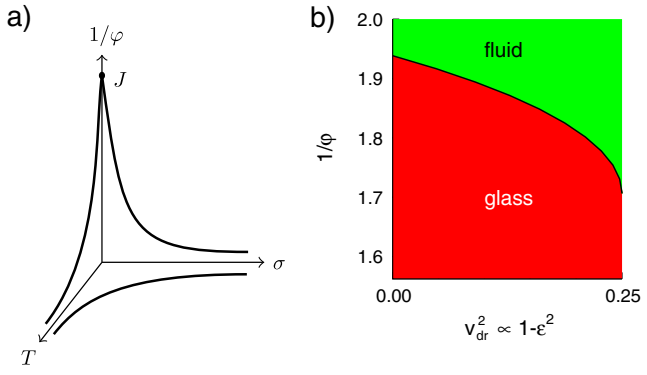

FIG. 1 (color online). (a) The jamming diagram for sheared systems as a function of inverse packing fraction φ^{-1}, temperature T, and shear stress σ. (b) Jamming diagram for driven inelastic hard spheres where the driving power v_{dr}^2 replaces the shear stress. In this latter case, the temperature dependence is trivial for $T > 0$, and the origin of the graph lies at random-close packing.

 © 2010 The American Physical Society

collision frequency to keep the energy constant. The driving amplitude, v_{dr}, is fixed and the direction of the kick, $\boldsymbol{\xi}_i(t)$, is chosen randomly from a Gaussian distribution, $P(\boldsymbol{\xi})$, with unit variance. To ensure momentum conservation, we choose pairs of neighboring particles and kick them in opposite directions [12]. A stationary state is reached, when the energy loss due to collisions is balanced by the energy input due to driving. Hence it is the driving power, $P_{\mathrm{dr}} = m v_{\mathrm{dr}}^2 \omega_{\mathrm{dr}}/2$, which determines the kinetic granular temperature, $T = m\langle \boldsymbol{v}^2\rangle/3$, according to

$$(1-\epsilon^2)\omega_{\mathrm{coll}} T = 8P_{\mathrm{dr}}. \tag{1}$$

Here $\omega_{\mathrm{coll}} \propto \sqrt{T}$ is the elastic collision frequency. In the following, the theory is formulated for arbitrary dimensions, and numerical results are presented for three dimensions.

The time evolution of the system consists of ballistic motion in between binary collisions and random kicks. These can be formally incorporated in a pseudo-Liouville operator $\mathcal{L}_+$ [11,13], which generates the time evolution of an observable, such as the density

$$\rho_q(t) = \frac{1}{N}\sum_i \exp[i\boldsymbol{q}\cdot\boldsymbol{r}_i(t)] = \exp(it\mathcal{L}_+)\rho_q(0).$$

For the discussion of the long-time dynamics, the central quantity of interest is the density correlation function,

$$\begin{aligned} F(q,t) &= \int d^3\xi P(\boldsymbol{\xi}) \int d\Gamma w(\Gamma)\rho_q^*(0)\rho_q(t) \\ &=: \langle \rho_q(0)|\rho_q(t)\rangle, \end{aligned}$$

which is directly accessible from computer simulations and experiments. Here, $w(\Gamma)$ is the stationary N-particle distribution and $\Gamma = \{\boldsymbol{r}_i, \boldsymbol{v}_i\}_{i=1}^N$ denotes a point in phase space.

Following Mori and Zwanzig, the normalized correlation function, $\phi_q(t) = F(q,t)/S(q) = F(q,t)/F(q,0)$, can be represented in terms of restoring forces (ν_q, Ω_q) and a memory kernel (M_q) [14],

$$(\partial_t^2 + \nu_q\partial_t + \Omega_q^2)\phi_q(t) = -\int_0^t d\tau M_q(t-\tau)\partial_\tau\phi_q(\tau). \tag{2}$$

The representation in Eq. (2) is exact. It correctly accounts for the conservation laws for the density, $\rho_q(t)$, and the longitudinal momentum, $q j_q^L(t) = \partial_t \rho_q(t)$. Energy is not conserved in a granular medium and transverse momentum is decoupled. Hence, the representation guarantees the correct hydrodynamic limit of $\phi_q(t)$. The restoring forces are given by the hydrodynamic fields

$$\nu_q = \frac{N}{v_0^2}\langle j_q^L|\mathcal{L}_+ j_q^L\rangle, \qquad \Omega_q^2 = \frac{N^2}{v_0^2 S_q}\langle \rho_q|\mathcal{L}_+ j_q^L\rangle\langle j_q^L|\mathcal{L}_+\rho_q\rangle.$$

The thermal velocity $v_0 = \sqrt{T/m}$ and initial conditions are $\phi_q(0) = 1$, $\partial_t\phi_q(0) = 0$.

Detailed balance does not hold and consequently, the transition rates of forward and backward reactions are not simply related, $\langle \rho_q|\mathcal{L}_+ j_q^L\rangle \neq \langle j_q^L|\mathcal{L}_+\rho_q\rangle^*$, as it would be the case in equilibrium systems. For the same reason, the memory kernel, $M_q(t) = \langle R_q^\dagger|R_q(t)\rangle$, is now given by the *cross* correlation of two unequal fluctuating forces, $R_q \neq R_q^\dagger$, driven by the reduced dynamics. Details of the calculation can be found elsewhere [15].

To proceed, we have to resort to approximations. First, we need an approximate form of the N-particle distribution to compute static (equal time) correlations. We assume that positions and velocities are uncorrelated $w(\Gamma) = w_r(\{\boldsymbol{r}_i\})w_v(\{\boldsymbol{v}_i\})$ and that the velocity distribution factorizes into a product of one-particle distributions, $w_v(\{\boldsymbol{v}_i\}) = \prod_i w_1(\boldsymbol{v}_i)$. The precise from of $w_1(\boldsymbol{v})$ is not needed, it only has to satisfy $\langle \boldsymbol{v}\rangle = 0$ and $\langle \boldsymbol{v}^2\rangle = 3T/m < \infty$. Furthermore, the system is assumed to be isotropic and homogeneous except for the excluded volume: $w_r(\{\boldsymbol{r}_i\}) = \prod_{i<j}\theta(r_{ij} - d)$. We find

$$\begin{aligned} \nu_q &= -i\omega_E \frac{1+\varepsilon}{2}[1 - j_0(qd) + 2j_2(qd)], \\ \Omega_q^2 &= \frac{q^2 v_0^2}{S_q}\left(\frac{1+\varepsilon}{2} + \frac{1-\varepsilon}{2}S_q\right), \end{aligned}$$

with ω_E the Enskog frequency for the elastic case and the spherical Bessel functions j_i.

An additional approximation is necessary to compute the memory kernel. The success of MCT for the description of dense molecular and colloidal fluids motivates its application also to dissipative granular fluids. First, we project the fluctuating forces onto products of densities. Second, the resulting higher order correlations are factorized into pair correlations. Thereby, one generates an explicit expression for $M_q(t) = m_q(t)\Omega_q^2$ in terms of $\phi_q(t)$ [15],

$$m_q[\phi](t) \approx A_q(\varepsilon)\frac{nS_q}{q^2}\int d^3k V_{\boldsymbol{qk}}\phi_{\boldsymbol{k}}(t)\phi_{\boldsymbol{q-k}}(t) \tag{3}$$

with $V_{\boldsymbol{qk}}$ given by

$$V_{\boldsymbol{qk}} = S_{\boldsymbol{k}}S_{\boldsymbol{q-k}}[\hat{\boldsymbol{q}}\cdot\boldsymbol{k}c_{\boldsymbol{k}} + \hat{\boldsymbol{q}}\cdot(\boldsymbol{q}-\boldsymbol{k})c_{\boldsymbol{q-k}}]^2.$$

The direct correlation function, c_q, is related to the static structure factor via the Ornstein-Zernike equation $nc_q \equiv 1 - S_q^{-1}$ and $A_q(\varepsilon) = [1 + (1-\varepsilon)S_q/(1+\varepsilon)]^{-1}$ depends on ε explicitly. Inserting the mode-coupling approximation, Eq. (3), into Eq. (2), we get a self-consistency equation for $\phi_q(t)$. The only further input that is required is the static structure factor S_q. For simplicity, we use the elastic Percus-Yevick expression [14] here. Future work [15] will study the influence of a structure factor that depends on the coefficient of restitution ε.

A memory function under driving is not necessarily positive definite and might not even be a real function

[6,16]. Hence, it is surprising that for a driven granular fluid the only change compared to the elastic case is the ε-dependent prefactor $A_q(\varepsilon) > 0$; see Eq. (3). Consequently, the memory kernel itself is positive definite and all work devoted to the mathematical structure of the standard mode-coupling equations is readily applicable to the granular system; e.g., see [6] for a compilation. This finding is quite remarkable because it implies that a large number of results derived for equilibrium systems also holds for a system far from equilibrium. In particular, a positive definite memory function in Eq. (3) guarantees non-negative spectra. On the other hand, the well-established universality of glassy dynamics (i.e., independence from the microscopic dynamics) is broken for granular fluids since the memory kernel depends on ε explicitly.

A glass transition is signaled by the appearance of a time-persistent part of the density correlations $f_q := \lim_{t\to\infty}\phi_q(t)$ in Eq. (2). In this limit, Eq. (2) reduces to the algebraic equation $f_q/(1-f_q) = m_q[f]$ which is solved readily by standard procedures [17]. For all values of the coefficient of restitution, $0 \le \varepsilon \le 1$, an ideal glass transition of the driven granular fluid is found with a transition density $\varphi^c(\varepsilon)$, cf. Fig. 2. For increasing dissipation, i.e., smaller ε, the glass transition is shifted to higher densities. This can be understood as follows: for increased dissipation, $\varepsilon < 1$, the prefactor $A_q(\varepsilon)$ in Eq. (3) becomes smaller than unity. Dissipation and driving hence weaken the memory effects and destabilize the glass. This needs to be compensated by a higher density. The resulting compensation of enhanced dissipation and driving by increased density can be represented in a corresponding jamming diagram as shown in Fig. 1(b), where for simplicity the mean-field relation $v_{\mathrm{dr}}^2 \propto (1-\varepsilon)^2/4$ was used. It might be reassuring that, although the critical density increases with increasing dissipation, it stays below the density of random close packing.

The full dynamics of Eq. (2) is shown in Fig. 3 for a density close to the glass-transition density φ_c. $\phi_q(t)$ shows the generic two-step relaxation. After an initial fast relaxation, $\phi_q(t)$ approaches a plateau f_q in a critical decay, $\phi_q(t) - f_q \propto t^{-a}$. The variation of the critical exponent a is shown in the inset of Fig. 2. For values below the transition, $\varphi < \varphi^c$, a second power law describes the decay from the plateau, known as the von Schweidler law, $\phi_q(t) - f_q \propto t^b$. The exponent b (not shown here) also varies with the coefficient of restitution ε, and is uniquely related to a.

At the transition point and beyond, $\varphi > \varphi^c$, the correlation function assumes a finite long-time limit $f_q > 0$ which sets in at a critical plateau value f_q^c. These values are shown in Fig. 4 for various values of ε. The increasing dissipation has three noticeable effects: (1) correlations at small wave numbers are enhanced, (2) oscillations reflecting the local structure become less pronounced, and (3) the localization length (indicated by the inverse of the width of the f_q distribution) decreases. The last finding is a consequence of the glass transition taking place at a higher density, cf. Fig. 2.

It was shown earlier that Newtonian (N) and Brownian (B) systems show the same glassy dynamics [7]. This is shown for the MCT dynamics in Fig. 5 for curves N and B, where N only needed to be shifted along the time axis to match B. In contrast, due to the explicit dependence on ε in Eq. (3), for any $\varepsilon < 1$, the granular long-time dynamics (G) cannot be scaled on top of the Newtonian or Brownian results. In addition, for granular dynamics at different ε there also exists no single master curve, cf. Fig. 3. Therefore, granular dynamics leads to a fundamentally different long-time behavior.

In conclusion, we have shown that MCT can be extended to granular fluids, which are in a steady state far from equilibrium. It can be shown that the resulting memory kernel in Eq. (3) is positive definite, and therefore most

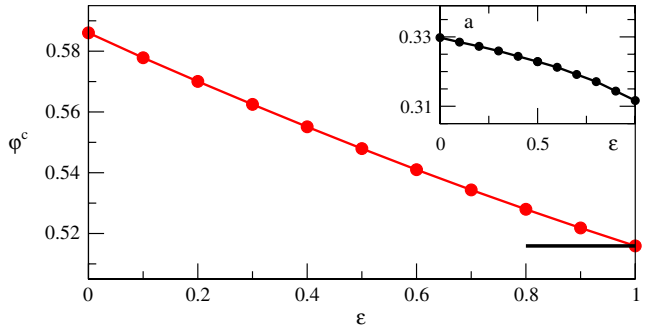

FIG. 2 (color online). Transition density φ^c as a function of the coefficient of restitution ε. The short horizontal bar indicates the result for the elastic case for $\varepsilon = 1$. The inset shows the evolution of the critical exponent a with ε.

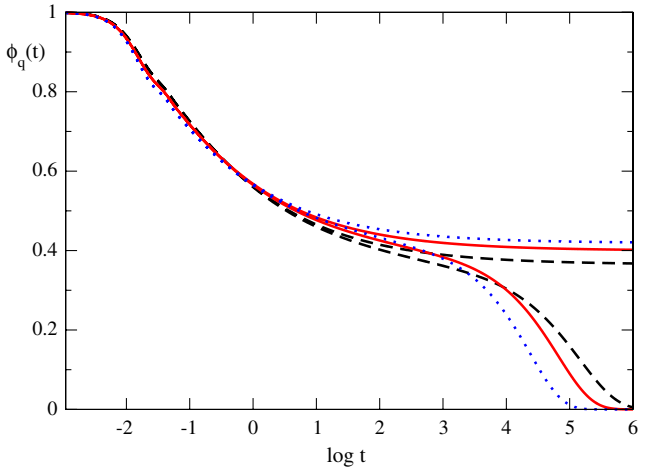

FIG. 3 (color online). Dynamics of the coherent density correlator $\phi_q(t)$ for the wave vector $qd = 4.2$ at the respective critical densities $\varphi^c(\varepsilon)$ and at $\varphi = 0.999\varphi^c(\varepsilon)$ for $\varepsilon = 1.0$ (dashed lines, elastic case), 0.5 (full lines), and 0.0 (dotted lines).

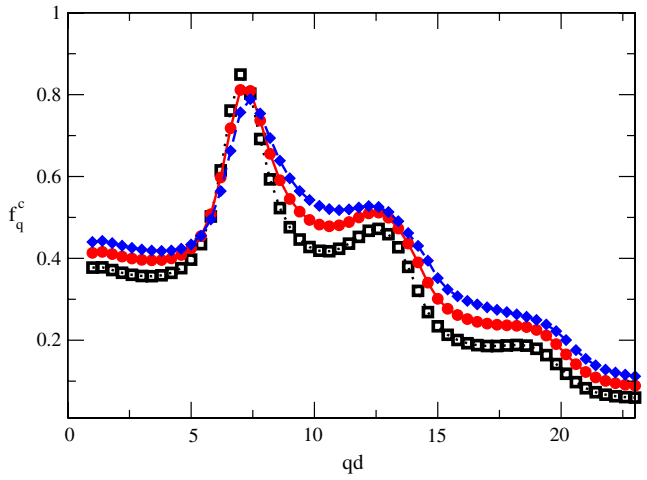

FIG. 4 (color online). Critical glass form factors f_q^c for coefficient of restitution $\varepsilon = 1.0$ (empty squares, elastic case), 0.5 (filled circles), and 0.0 (filled diamonds) as a function of wave number qd.

mathematical theorems from equilibrium MCT carry over to the driven granular case. An ideal glass transition is observed for all values of the dissipation or equivalently all values of the driving. Since the balance between dissipation and driving implies that the driving amplitude is proportional to the inelasticity $v_{\mathrm{dr}}^2 \propto (1-\varepsilon)^2$, the glass transition defines a line in the φ^{-1}-vs-v_{dr}^2 plane of a

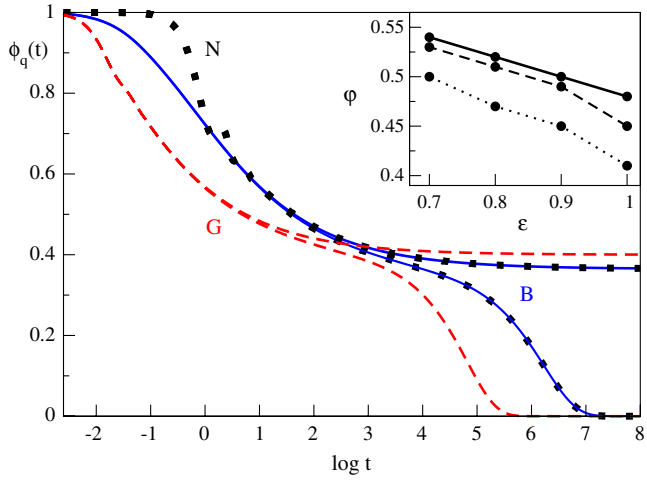

FIG. 5 (color online). Dynamic scattering function $\phi_q(t)$ for $qd = 4.2$ at the glass transition, $\varphi = \varphi_c$, and for slightly lower volume fraction, $\varphi = 0.999\varphi_c$ for Newtonian dynamics (N, dotted curves) with $\nu_q = 0$, Brownian dynamics (B, full curves), and granular dynamics (G, dashed curves) with coefficient of restitution $\varepsilon = 0.5$. The Newtonian dynamics is scaled along the time axis to match the Brownian dynamics at long times. No such rescaling is possible for the granular dynamics. The inset shows three lines of equal diffusivity (from top to bottom: $D = 0.7$, 0.8, and 0.9 in relative units) taken from the data of a computer simulation [12].

generalized jamming diagram, cf. Fig. 1. The universality known for Newtonian and Brownian dynamics is broken in the granular case; however, the predicted differences in the critical exponents, cf. inset of Fig. 2, and glass form factors, cf. Fig. 4, are relatively small. Comparably large changes with increased dissipation are expected in the transition densities as shown in Fig. 2. This prediction can be supported by looking at a precursor of the glass-transition line in computer simulation data: For increasing dissipation, points of equal diffusivity are found to be shifted to higher densities (inset of Fig. 5) in accordance with our predictions for the glass transition in Fig. 2. Therefore, we expect our results to be testable in further computer simulation studies and also in experiments. Without rigorous proof we expect the presented results to apply also to variations of the driving mechanism. While shearing might be a different case, cf. [8], thermalizations similar to the ones described above can be expected to exhibit similar results.

We thank T. Aspelmeier, A. Fiege, and J. Horbach for interesting discussions. This work was supported by DFG Sp714/3-1, BMWi 50WM0741, and DFG FG1394.

[1] A. Liu and S. R. Nagel, Nature (London) **396**, 21 (1998).
[2] C. S. O'Hern, L. E. Silbert, A. J. Liu, and S. R. Nagel, Phys. Rev. E **68**, 011306 (2003).
[3] U. Bengtzelius, W. Götze, and A. Sjölander, J. Phys. C **17**, 5915 (1984).
[4] W. van Megen and P. N. Pusey, Phys. Rev. A **43**, 5429 (1991).
[5] G. Szamel and H. Löwen, Phys. Rev. A **44**, 8215 (1991).
[6] W. Götze, *Complex Dynamics of Glass-Forming Liquids: A Mode-Coupling Theory* (Oxford University Press, Oxford, 2009).
[7] T. Gleim, W. Kob, and K. Binder, Phys. Rev. Lett. **81**, 4404 (1998).
[8] M. Fuchs and M. E. Cates, Phys. Rev. Lett. **89**, 248304 (2002).
[9] A. R. Abate and D. J. Durian, Phys. Rev. E **74**, 031308 (2006).
[10] P. M. Reis, R. A. Ingale, and M. D. Shattuck, Phys. Rev. Lett. **98**, 188301 (2007).
[11] T. Aspelmeier, M. Huthmann, and A. Zippelius, in *Granular Gases*, edited by T. Pöschel and S. Luding (Springer-Verlag, Berlin, 2001) pp. 31–58.
[12] A. Fiege, T. Aspelmeier, and A. Zippelius, Phys. Rev. Lett. **102**, 098001 (2009).
[13] M. Huthmann and A. Zippelius, Phys. Rev. E **56**, R6275 (1997).
[14] J.-P. Hansen and I. R. McDonald, *Theory of Simple Liquids* (Academic, London, 1986), 2nd ed.
[15] W. T. Kranz, M. Sperl, and A. Zippelius (to be published).
[16] I. Gazuz, A. M. Puertas, T. Voigtmann, and M. Fuchs, Phys. Rev. Lett. **102**, 248302 (2009).
[17] T. Franosch, M. Fuchs, W. Götze, M. R. Mayr, and A. P. Singh, Phys. Rev. E **55**, 7153 (1997).